

Photoemission study of CoO

Z.-X. Shen

Stanford Electronics Laboratory, Stanford University, Stanford, California 94305

J. W. Allen

Department of Physics, University of Michigan, Ann Arbor, Michigan 48109-1120

P. A. P. Lindberg, D. S. Dessau, B. O. Wells, and A. Borg

Stanford Electronics Laboratory, Stanford University, Stanford, California 94305

W. Ellis

Los Alamos National Laboratory, Los Alamos, New Mexico 87545

J. S. Kang

Department of Physics, University of Michigan, Ann Arbor, Michigan 48109-1120

S.-J. Oh

Department of Physics, Seoul National University, Seoul 151, Korea

I. Lindau and W. E. Spicer

Stanford Electronics Laboratory, Stanford University, Stanford, California 94305

(Received 29 January 1990; revised manuscript received 3 April 1990)

We have performed resonance photoemission, angle-resolved photoemission, and core-level photoemission studies of single-crystalline CoO. On the one hand, strong correlation effects among the d electrons are observed, as signaled by a strong reduction of Co $3d$ bandwidths and satellites in both the valence band and the cation core levels. On the other hand, the oxygen states are found to be very bandlike, as indicated by strong dispersions of oxygen states in the valence band and the lack of oxygen satellites. We give estimations of 30 and 1.5 for U/W (Coulomb interaction divided by bandwidth) ratio of Co $3d$ bands and O $2p$ bands, respectively. By comparing the experimental and theoretical E versus k relation, we show that the density-functional band calculation works well for the oxygen bands but not for the Co bands. We argue that CoO is not a band insulator, but a charge-transfer insulator. We have also observed the effects of local magnetic order on the electronic structure. Finally, we suggest a guideline on calculating the band structure of CoO: introducing a mechanism that reduces the Co $3d$ bandwidth by 25% while still retaining the other essential features of the band calculation.

I. INTRODUCTION

Stimulated by the discovery of cuprate superconductors,¹ the electronic structure of the transition-metal oxides has once again become a focal point for the condensed-matter physics community.² Due to their simpler structures, the transition-metal mono-oxides like NiO and CoO provide opportunities for a better understanding of the electronic structure of these highly correlated materials, which is clearly a key to microscopic theories of high-temperature superconductivity. For the past 50 years, the insulating nature of these transition-metal mono-oxides, so-called "Mott insulators," has been a continuing problem for the condensed-matter physics community.³ Currently, there are two different viewpoints held by different parties in this dispute.⁴ The first group, initiated by Mott, Hubbard, and Anderson, views the failure of the band theory to predict the insulat-

ing nature of these oxides as due to an intrinsic limitation of the one-electron approach: using the charge distribution of the ground state to calculate the energies of the excited states.⁵⁻⁹ The second group, originating with Slater, argue that this failure of band theory is due to certain approximations used in the calculations instead of the band theory itself.¹⁰ They believe that the band calculations should be able to describe the electronic structure of the transition-metal mono-oxides well. In fact, a recent sophisticated band calculation gave a semiconducting nature for NiO, a result viewed by the second group as a great triumph for the band theory.¹¹ From the standpoint of the second group, it is essential to include the antiferromagnetic order in the calculation, which, in its original form, expects a metal-insulator transition at the Neel temperature (T_N).

Due to historical reasons, NiO and CoO have been the most important Mott insulators, with respective band

gaps of 4 and 6 eV.¹² Both of them show antiferromagnetic transitions, at temperatures of 525 and 289 K, respectively.^{13,14} After extensive experimental and theoretical studies on NiO and Ni dihalides, especially due to recent spectroscopic works, NiO has been established to be a charge-transfer insulator with about 4 eV energy gap and a strong *d-d* correlation energy U_d of 8 eV.^{8,9,15} On the other hand, however, very few spectroscopic experiments have been performed to explore the band effects of NiO. Recently, angle-resolved photoemission studies have been performed to investigate the effects of translational symmetry on the electronic structure of these oxides.^{16,17}

Relatively speaking, much less attention has been paid to CoO as compared with NiO.^{18–20} Unlike NiO, CoO has an odd number of electrons per unit cell, which makes it more difficult for the band theory to reconcile its insulating nature. Nevertheless, Terakura *et al.* suggested that by using the Slater antiferromagnetism approach (each unit cell contains two CoO molecular units so that the number of electrons per unit cell is even), the band theory will be able to give an insulating ground state.¹¹ Even though their results show a metallic nature for CoO in both paramagnetic and antiferromagnetic phases, they argued that it is caused by a spin imbalance and a poor treatment of the exchange energy, not the band calculation itself. An important consequence of the spin-polarized band calculation is that the electronic structures of the paramagnetic and antiferromagnetic phases are very different.^{11,21,22} A possible way to test the validity of this approach is to perform photoemission spectroscopy (PES) experiments to measure and compare the electronic states in the paramagnetic and antiferromagnetic states. However, such an experiment has been proven to be difficult to perform on NiO. Earlier work on NiO by Powell and Spicer found that the NiO decomposed in vacuum when it is heated up to its T_N , 525 K.²³ Fujimori *et al.* have recently performed such a study on polycrystalline NiS without finding any difference between valence-band photoemission spectra recorded at paramagnetic and antiferromagnetic states, even though the calculated density of states differs drastically.²²

In this paper, we report results of our photoemission studies of CoO single crystals, which includes Co resonance photoemission, x-ray photoemission, and angle-resolved photoemission. On the one hand, strong correlation effects were observed. Co satellites were observed both in the valence band and Co core levels, with the Co character of the valence satellite verified by its resonance behavior. Such satellites cannot be explained by one-electron band calculations. The Co *3d* bandwidth obtained from angle-resolved photoemission data is only about 25% that of the bandwidth from one-electron band calculations. Following the example of NiO,⁸ we interpret the resonance photoemission data in terms of a cluster configuration interaction model derived from the Anderson lattice Hamiltonian. We argue that CoO is a charge-transfer insulator instead of a band insulator. On the other hand, we find that the experimental E versus k relation for oxygen bands agree with the results of a band calculation very well. This receives support from the fact

that no oxygen satellite was observed, which cannot be reconciled within the framework of the cluster model. Finally, we found that one has to include the effects of local magnetic orders on the electronic structure in order to reconcile the angle-resolved photoemission data, which is consistent with results of x-ray photoemission spectroscopy (XPS) measurements above and below its T_N . We point out that the fact no change of photoemission spectra above and below T_N cannot by itself disprove the validity of the band calculation.

This paper is organized in the following way. Section II gives details of experimental set-ups. Section III gives the results of resonance photoemission, core-level XPS data, and a cluster-model interpretation of these data. Section IV gives results of photoemission studies of CoO above and below its Neel temperature. Section V gives results of angle-resolved photoemission studies of CoO and its comparison with the predictions of one-electron band calculations. Section VI summarizes our results.

II. EXPERIMENTAL

The photoemission data were obtained from three different chambers on two different lines at the Stanford Synchrotron Radiation Laboratory (SSRL). In all cases, a single-crystalline sample of CoO was transferred into the chamber and cleaved *in situ* to expose a (001) face, which shows a sharp, square pattern by a low-energy electron diffraction (LEED) measurement.

The Co resonance photoemission data were recorded at the 4th beam line at SSRL using a vacuum chamber with a base pressure of 2×10^{-10} Torr. A commercial double-pass cylindrical mirror analyzer (CMA) was used as an electron-energy analyzer. The overall energy resolution from both the analyzer and the photon source is about 0.4 eV in the photon energy range.

The temperature dependence of the PES and LEED data were measured in a Varian photoemission chamber with a base pressure of 3×10^{-10} Torr. A helium discharge lamp, a Mg (1253.6 eV), and a Zr (151.4 eV) x-ray source were used to excite the photoelectrons which were analyzed by a (CMA). The overall resolutions for spectra taken at 40.8, 151.4, and 1253.6 eV were 0.4, 1.2, and 1.2 eV, respectively. The temperature of the sample was monitored by a thermocouple attached to the back of the sample holder. Due to the insulating nature of the compound, the sample surface was charged up during the XPS measurements. However, the charging was stabilized and did not affect the line shape, which was verified both by repeating the measurement and by comparing with earlier published data.¹⁸ The binding energies of the XPS spectra in Figs. 4 and 5 and in Table I were determined by comparing the Co *2p* core level with established data.¹⁸ This will not affect our discussion because we will only focus on line shapes and relative positions of the different peaks. The room-temperature ultraviolet photoemission spectroscopy spectrum does not seem to be charging,¹⁹ where the Fermi level was referenced to a gold film evaporated *in situ*. Similar LEED patterns were observed for the sample at different temperatures.

The angle-resolved photoemission experiment was per-

TABLE I. Binding energies of various core levels of CoO.

	(eV)
Co 2p _{3/2} (<i>m</i>)	-780.0
Co 2p _{3/2} (<i>s</i>)	-786.0
Co 3p(<i>m</i>)	-60.6
Co 3p(<i>s</i>)	-64.9
Co 3s(<i>m</i>)	-102.2
Co 3s(<i>s</i>)	-106.5
O 1s	-528.5
O KVV Auger	512.4 (kinetic energy)

formed on the Seya-Naminoka beam line III-2 using photon energies between 10 and 35 eV. All measurements were carried out in a VG ADES 400 system equipped with a hemispherical analyzer operating with angular resolution of $\pm 2^\circ$. The combined energy resolution from the analyzer and the photon source is better than 0.3 eV for $h\nu < 27$ eV. The chamber base pressure was 1×10^{-10} Torr. The Fermi-level position was determined by a metal-reference spectrum. The experiments were performed at room temperature with CoO in its paramagnetic phase. The photoelectrons were collected at normal emission. Unless otherwise stated, the 45° photon incident angle is used, giving mixed *s* and *p* polarizations and relaxed selection rules.

III. RESONANCE AND CORE-LEVEL PHOTOEMISSION STUDIES OF CoO

A powerful way to understand the features of valence-band photoemission spectra is to perform resonance photoemission experiments. During the past decade, resonance photoemission experiments have been extensively used to study the transition-metal compounds,²⁴⁻²⁶ including recent works on high-temperature superconductors.²⁷⁻³⁰ Resonance photoemission is a phenomenon of enhancements or suppressions of photoemission features due to a new emission channel of super-coester-croning Auger decay. For CoO, resonance photoemission involves two channels:

$$3p^6 3d^7 + h\nu \rightarrow 3p^6 d^6 + e,$$

$$3p^6 3d^7 + h\nu \rightarrow 3p^5 3d^8 \rightarrow 3p^6 3d^6 + e.$$

The first channel is the direct photoemission channel, while the second channel, which will open as the photon energy reaches the 3p to 3d absorption threshold, is a Auger decay following a photoabsorption process. The final state of the two channels are indistinguishable so that there is a quantum interference between the two channels. As a result of the interference, the Co features are enhanced or suppressed at the absorption threshold near 60 eV.

Figure 1 shows the energy-distribution curves of CoO at photon energies near 60 eV. The photoemission spectra were aligned with respect to the valence-band maxima. Comparing the spectra taken at 60 and 61 eV photon energies, one can easily tell that feature B shows a

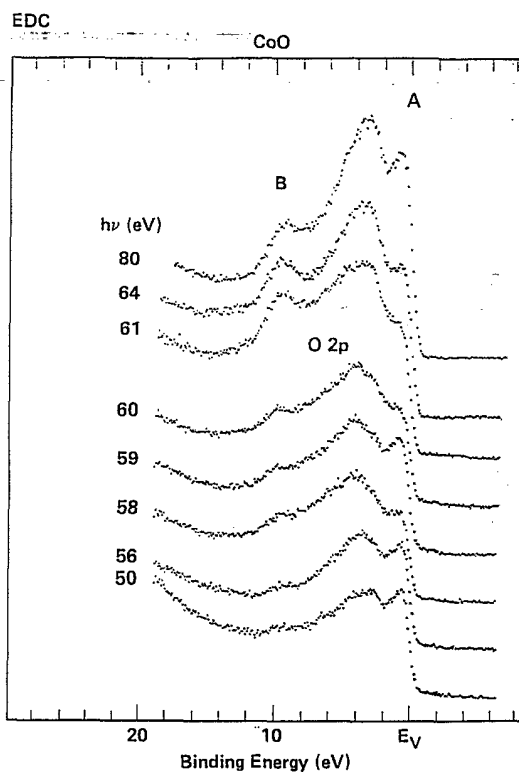


FIG. 1. Angle-integrated energy-distribution curves of CoO at photon energies near Co 3p to 3d absorption threshold of 60 eV. All the curves are matched to each other with respect to their valence-band maximum. The satellite (peak B) shows a clear resonance at 61 eV.

clear enhancement. This indicates that it exhibits a resonance behavior and is a Co feature. This feature, which we assign to be a Co 3d⁶ satellite, is not predicted by an one-electron band calculation,¹¹ and is often taken to be a signal of strong correlation effects. Another way of performing a resonance photoemission experiment is to take so called constant-initial-state (CIS) measurements, which basically reflect the photoemission intensity as a function of photon energies. The upper and the lower panels of Fig. 2 present CIS curves of "peak A" and "peak B," respectively. An enhancement of the photoemission spectra is clearly observable at 61 eV for both peaks. The fact that both peak A and peak B shows resonance is somewhat unusual, because in most of the transition-metal compounds, the main band exhibits a "antiresonance" while the satellite exhibits a resonance.^{25,28} Examining the curves more carefully, one finds that there are two resonance structures, a smaller one at 59.5 eV followed by a larger one at 61 eV. This behavior is different from the Ni resonance in NiO.²⁵ The origin of this double enhancement structure in the CIS curve remains unclear, however, a very likely explanation is that this is caused by transitions from the two spin-orbital components of the Co 3p initial state.

The PES spectra of CoO have been interpreted in terms of a crystal-field splitting,¹⁸⁻²⁰ and were also inter-

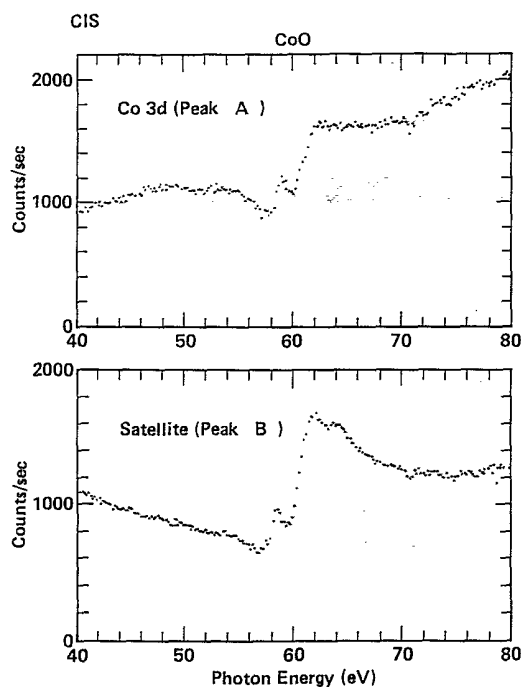


FIG. 2. Angle-integrated CIS curves of the two main valence-band features *A* and *B* of Fig. 1. The upper and the lower panels give the results of peaks *A* and *B*, respectively. Both of them show a small resonance at 59.5 eV, followed by a larger resonance at 61 eV.

preted to give a 2 eV value for U_d ,³¹ which was viewed as a strong evidence to support the band approaches.³² In light of the new understanding of the NiO PES data^{8,9,15} as well as the CoO resonance photoemission data, these interpretations appear to be inconsistent. The main difficulty for these interpretations is that they cannot explain the Co 3*d* satellite *B* and its resonance behavior very well. Following the scheme developed for NiO, we try to understand the electronic structure by a cluster model, where a cluster of $(\text{CoO}_6)^{-10}$ is treated as a separable unit. Such a model, which takes both the correlation energy U_d and *p-d* charge-transfer energy Δ into account explicitly, has been proven to be a successful model to interpret the PES spectra of the highly correlated compounds.^{8,9,15} In the spectrum of Fig. 3, the features extending from -3 to -7 eV are mainly oxygen states, which will be discussed in more detail in Sec. V. Peak *A*, which was interpreted earlier as due to the Co 3*d*⁶ states,^{19,31} is assigned to be d^7L , where *L* stands for ligand hole states. Since the optical gap, which we believe is due to predominantly $d^7 + d^7 \rightarrow d^7L + d^8$ intra-cluster transitions, is about 6 eV,¹² we predict that the first inverse photoemission peak d^8 will be located near 4 eV above E_F . Considering the ground state and final-state hybridization shifts, 5–7 eV is a reasonable estimate for Δ . Peak *B* is assigned to a d^6 satellite as suggested by the resonance photoemission data presented in Figs. 1 and 2. The approximately 14.5 eV separation between d^6 and d^8 configurations reflects the size of U_d . Taking into

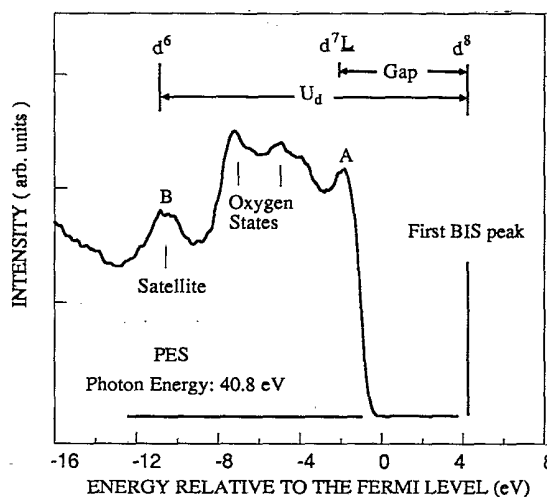


FIG. 3. Valence-band angle-integrated photoemission spectra with a cluster configuration interaction model interpretation. The Fermi level is determined by a metal reference spectra, and the position of the first bremsstrahlung isochromat spectroscopy (BIS) peak is extrapolated from optical-absorption data (Ref. 23).

account the uncertainties of the ground and final states hybridization shifts, we believe 9–11 eV U_d is a fair estimate for U_d .

It is worthwhile to point out here that these values of U_d and Δ are consistent with the magnetic properties of CoO. In their discussion of the superexchange interaction for NiO, CoO, FeO, and MnO, Zaanen and Sawatzky derived a formula for the superexchange energy, $J \sim (1/\Delta + 1/U_d)$.³³ Assuming a similar hybridization energy for CoO and NiO, it is easy to understand why, as a result of the larger Δ and U_d , CoO has a lower antiferromagnetic transition temperature (smaller *J*) than NiO.⁸

As has been established in many transition-metal (TM) compounds, the line shape of the TM 2*p* core level is very sensitive to the electronic structure of the compound.³⁴ The lower panel of Fig. 4 shows Co 2*p* core-level XPS spectra. In addition to the two-spin orbital components, two satellites were observed in the Co 2*p* core-level spectra. We have tried to fit the $2p^{3/2}$ spin-orbital component by a main and a satellite Gaussian, but the result was unsatisfactory, which indicates that a more sophisticated approach is needed to fit the line shape of Co 2*p* core level. However, we can determine the energy separation between the main line and the satellite is about 6 eV, which is consistent with the values of Δ and U_d determined from the valence-band spectra. According to the cluster model,¹⁵ the energy separation of the main line and the satellite is $U_{cd} - \Delta$ without considering the hybridization shifts, where U_{cd} is the Coulomb interaction between a *d* hole and a 2*p* core hole. Given the size of U_d , 11–13 eV U_{cd} will be a very reasonable value,³⁵ yielding the measured 6 eV separation for the main line and the satellite of the Co 2*p* core level. It should be noted that the values

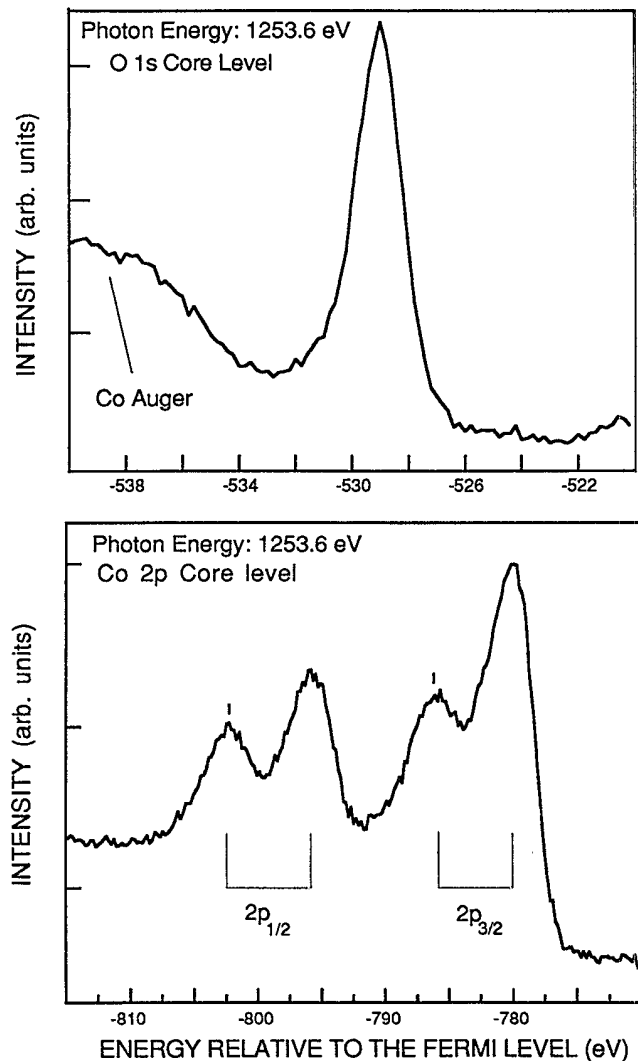


FIG. 4. X-ray photoemission data of O 1s and Co 2p core levels of CoO. A clear difference is that the Co 2p core level has satellites while the O 1s core level does not have a satellite. The broad structure at the higher binding energy side of the O 1s core level is due to the Co Auger spectrum.

of Δ in the valence band and core-level fitting are in principle different.³⁶ However, since we are only doing a rough estimation, we ignore their difference at this level of accuracy.

In principle, satellites structures are expected to be observed in all the cation core levels in the large- d transition-metal mono-oxides, but there are very few reports of these in the literature except 2p core levels. In Table I, we list the binding energies of main lines and their satellites of the Co core levels.³⁷ Following similar arguments as for the Co 2p core level, we can estimate the Coulomb interaction between a d hole and a core hole for the different core levels. The estimated model parameters are listed in Table II. Table I also lists the binding energy of the O 1s core level and the kinetic energy of O KVV Auger electrons. The difference between the bind-

TABLE II. The parameters obtained for the cluster model. Δ is the charge-transfer energy between a 3d hole and a 2p hole. U_d is the Coulomb interaction of two d holes, $U_{cd}(2p)$, $U_{cd}(3s)$, and $U_{cd}(3p)$ are the Coulomb interactions between a 3d hole and a 2p core hole, 3s core hole and 3p core hole, respectively. U_p is the Coulomb interaction between two oxygen p holes. W_d and W_p are bandwidths for the Co 3d and O 2p bands, respectively.

	(eV)
Δ	5-7
U_d	9-11
$U_{cd}(2p)$	11-13
$U_{cd}(3s)$	9-11
$U_{cd}(3p)$	9-11
U_p	~ 6
W_p	4
W_d	0.3

ing energy and the kinetic energy is about 16 eV, which equals the Coulomb repulsion U_p between two p holes plus the binding energies of the two oxygen valence holes. Taking the average binding energy of oxygen states in the valence band to be -5 eV, we obtain a value of 6 eV for U_p . Another important observation one can make from Table I is that there are no obvious satellites in the O 1s core level, which is shown more clearly in the lower panel of Fig. 4. The large broad structure at the higher binding energy to the O 1s core level is due to a Co Auger process. Given the fact that U_p is as large as 6 eV (of the same order as U_d), one cannot reconcile this absence (or very weak, if any) of the satellite structure of the O 1s core level within the framework of the cluster model. However, it would be easier to understand this difference between the observation of satellites in the Co core levels and the absence of satellite in the O 1s core level if one takes into account the differences of the bandwidth between the Co and O valence states. The measured widths for Co 3d and O 2p bands are 0.3 and 4 eV, respectively, as we will show in Sec. V.

IV. PHOTOEMISSION MEASUREMENTS ABOVE AND BELOW T_N

An important consequence of the spin-polarized band calculation is that the electronic states of the compound in the paramagnetic phase and the antiferromagnetic phase are very different. In the original idea of spin-polarized band calculation, a metal-insulator transition is expected at T_N .¹⁰ A possible way to test the validity of this approach is to perform PES experiments to measure and compare the electronic structures of transition-metal mono-oxides in the paramagnetic and antiferromagnetic phases. Such an experiment has been proven to be difficult to perform on NiO since it decomposes in vacuum at its Neel temperature of 525 K.²³ However, it is possible to perform such an experiment on CoO whose Neel temperature is just below the room temperature.

Figure 5 presents experimental data of CoO recorded at 100 and 300 K where CoO is in its antiferromagnetic and paramagnetic phases, respectively. (a) and (b) show

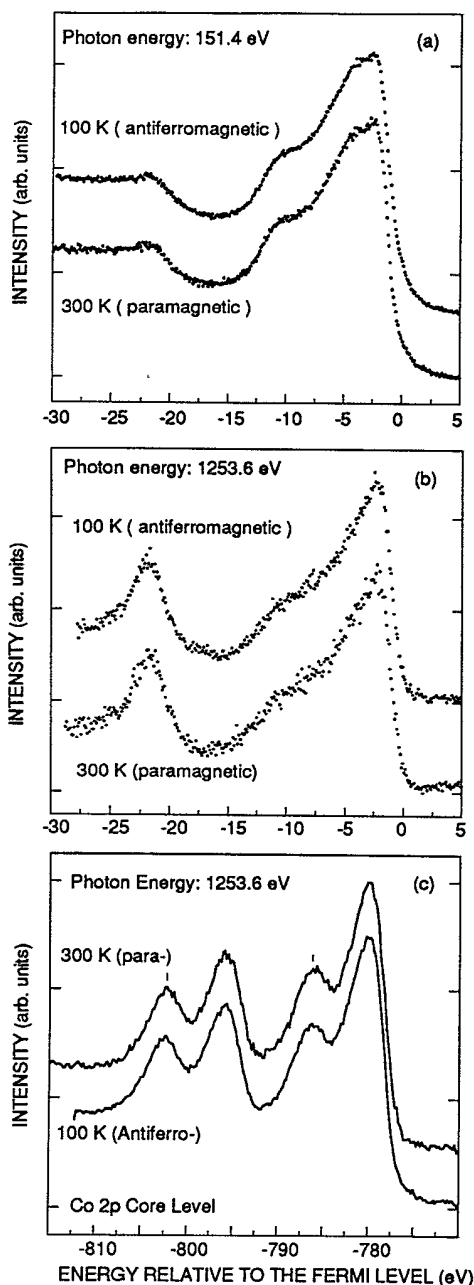


FIG. 5. Valence-band and core-level photoemission spectra recorded at paramagnetic and antiferromagnetic phases of CoO. (a), (b), and (c) show valence-band spectra at 151.4 eV photon energy, valence-band spectra at 1253.6 eV photon energy, and Co 2*p* core-level spectra at 1253.6 eV photon energy.

valence-band spectra taken at two different photon energies: 151.4 and 1253.6 eV, respectively, and (c) shows the Co 2*p* core level. The photoemission spectra taken at the two phases of CoO are identical, i.e., no electronic structure change was observed in the XPS spectra when the sample went from the paramagnetic phase to the antiferromagnetic phase. This result is in contrast to the simple picture of a metal-insulator transition at T_N expected from the band calculations by assuming that the spins are

at completely random orientations above T_N .^{10,11} A similar result has been obtained from NiS by Fujimori *et al.* which they suggest was a sign of failure of the band calculation.²² However, one has to be cautious in drawing a conclusion based on data obtained by an experimental technique which is neither spin polarized nor angle resolved, such that it is not sensitive to the spin order. For example, no LEED superstructure was observed when the CoO sample went from its paramagnetic phase to its antiferromagnetic phase, in contrast to what one would expect if the electron beam was sensitive to the spin order. A possible explanation is the following: even in the paramagnetic phase, there still exists local spin order within certain domains (like the ferromagnetic situation) such that the paramagnetic phase looks like the antiferromagnetic phase when probed by PES, which is a local probe and insensitive to the spin.

Effects of magnetic order on photoemission spectra were also investigated in ferromagnets. Angle-integrated photoemission spectra of Ni and Fe were measured above and below their Curie temperatures, and they were found to be exactly the same.³⁸⁻⁴⁰ These results are in contrast to a simple itinerant band model, which predicts a clear difference in the total density of states above and below the Curie temperature due to the so-called exchange splitting.⁴⁰ Several theoretical arguments were proposed to explain the seemingly inconsistent results. Slater pointed out that the energy splitting between the spin-down and spin-up electron bands has no connection with the Curie temperature, and thus no change should be observed above and below the Curie temperature.⁴¹ A simple model was suggested by many authors where a local moment is formed on each atom, which persists but is disordered above the Curie temperature.⁴² The difference in the total density of states should be of the order of kT_c rather than the so-called exchange splitting, hence, no large change of the total density of states should be expected. Recently, an angle-resolved photoemission experiment has been performed on Ni(111) surface by Eastman *et al.* which showed some changes in the photoemission spectra below and above the Curie temperature.⁴³ Most importantly, this experiment has also demonstrated a nonvanishing exchange splitting above the Curie temperature, which is in contrast to the long-range-order models such as the simple Stoner-Wohlfarth-Slater model which predicts that the exchange splitting disappears above the Curie temperature.⁴⁴ Several theoretical approaches of itinerant electron ferromagnetism have been proposed to explain this observation.⁴⁵⁻⁴⁹ The basic ideas of these approaches are similar: a typical magnetization configuration, although it may be time dependent and without any long-time or long-range order, will still possess significant short-range order. Locally the average magnitude of the magnetization is not much different from that in the absolute zero of temperature. The short-range magnetic order then allows a definition of "local bands" which are exchange split with respect to the local direction of magnetization. This way, they can at least qualitatively understand the experimental finding that the exchange-splitting is nonvanishing above the Curie temperature. Recently, the temperature dependence

of the exchange splittings in Ni and Fe was investigated by spin-resolved photoemission experiments.^{50,51} The results of these experiments suggest that the effect of spin on spin-resolved PES spectra is important, and a pure Stoner model cannot explain the experimental data (in other words, short-range magnetic order persists above the Curie temperature). These results are consistent with the spin-unresolved photoemission studies. From the above discussions, it is very clear that the local magnetic order is essential to the electronic structure of the ferromagnets just above their Curie temperature. Thus, it is very conceivable that the local magnetic order is also important to the electronic structure of antiferromagnets just above their Neel temperature.

This notion of the existence of a short-range magnetic order above T_N also finds its support from recent experiments of photoelectron diffraction of Mn compounds.^{52,53} Data at kinetic energy near 100 eV for the spin-split Mn 3s multiples show almost no changes in the $^5S:7S$ intensity ratio at T_N , but show abrupt changes at 4.5 times and 2.7 times T_N for MnO and KMnF₃, respectively. Such sharp transitions are speculated as due to phase transition of local magnetic order. This clearly suggests the existence of a short-range magnetic order in the Mn compounds above T_N , and it is very reasonable to believe a similar magnetic order exists in CoO. As a matter of fact, Hermsmeier *et al.* noted that the transition temperatures of these short-range magnetic order transition are very close to the relevant Curie-Weiss constants.⁵² They speculated that the short-range magnetic order might be completely destroyed above the corresponding transition temperatures. It would be very interesting to perform PES, especially angle-resolved PES, above and below these transition temperatures. It should be pointed out that Hermsmeier *et al.* has observed a 0.4 eV narrowing in photoemission spectra of MnO when the temperature is cooled down below its Neel temperature.⁵⁴ This is clearly different with our CoO data and the NiS data of Fujimori *et al.*,²² more systematic photoemission studies of transition-metal compounds above and below their Neel temperature are needed to understand this observed difference.

V. ANGLE-RESOLVED PHOTOEMISSION STUDY

As we have indicated in Sec. III, the simple cluster model cannot explain all the experimental data even though it explains the satellite structures in the valence band and the Co core levels very nicely. Naturally, the cluster model ignores completely the band effects which certainly are important aspects of the electronic structure of solids. A powerful way to explore the band effects is to perform angle-resolved photoemission experiments.⁵⁵ In an angle-resolved photoemission experiment the photoemitted electrons are analyzed with respect to both their kinetic energy and their direction of propagation. Since the wave-vector component parallel to the sample surface is conserved at the solid-vacuum interface, angle-resolved photoemission spectroscopy allows the initial-state energies to be mapped out as a function of the parallel component of the wave vector. In addition, at normal

emission, for which k_{\parallel} equals zero, the three-dimensional wave vector is confined to a symmetry line of the Brillouin zone. Thus, the experimental energy dispersions can be directly compared with band calculations that almost invariably are performed along high-symmetry axis. Symmetry information of the states can also be obtained if one changes the incident angle of the photon beam so that one changes the polarizations of the incident beam and thus the selection rules. For example, it has been shown that for a surface with fourfold symmetry, the final state that is probed in photoemission at normal emission has the full symmetry of the crystal surface.^{56,57} By symmetry, the integrand for the matrix element for the optical transition, $\langle \Psi_i | H_{\text{dipole}} | \Psi_f \rangle$, must be invariant under all symmetry operations or the matrix element will be zero. Thus the observed initial state must have the same symmetry as the dipole operator for the optical transition. The dipole operator is proportional to $e\mathbf{E}\cdot\mathbf{r}$ and has the symmetry of the electric-field vector of the incident radiation. With the fourfold symmetry like CoO(001), for incident light with an electric field parallel to the surface, the allowed initial states must have Δ_5 symmetry, while for incident light with an electric-field vector along the surface normal, the initial state must have Δ_1 symmetry.

Figure 6 presents angle-resolved photoemission data of a CoO(001) surface at normal emission with photon ener-

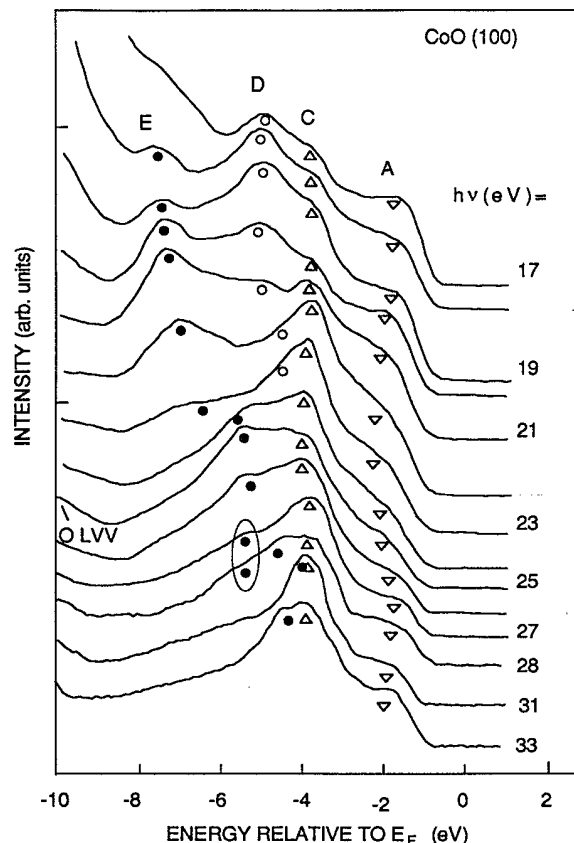


FIG. 6. Normal-emission angle-resolved photoemission data of the CoO(001) surface at photon energies from 17 to 33 eV.

gies from 17 to 33 eV. Four prominent features were identified in the data, which are labeled *A*, *C*, *D*, and *E*. The oxygen features *E* and *D* show clear dispersions as a function of photon energy. The feature *E*, which starts at its energy minimum at photon energies of 17–19 eV, shifts monotonically towards higher energy until 26 eV photon energy above which the situation becomes more complicated. It appears to turn back to lower energy slightly at 27 eV photon energy. This result is very similar to a result we obtained from NiO except the effect is weaker.¹⁶ We will come back and discuss this problem in detail later on, for now let us just state that it is not caused by reaching a critical point. (The *k* value calculated from this point is not corresponding to that of the Γ or *X* point.) Therefore, the feature *E* must continue to disperse upwards until it merges with features *D* and *C*, as indicated by solid circles. The feature *D* moves monotonically with the increasing photon energy towards

higher energy (lower binding energy) until it merges with the feature *C*, which remains basically nondispersive. The feature *A*, which is due to contributions from Co 3*d* states mixed with O 2*p* states having 3*d* symmetry with respect to Co ions, shows no strong dispersion.

As we have indicated earlier, we can find out information about the symmetry of valence states by recording photoelectrons at normal emission with different polarization of incident beams. Figure 7 presents normal emission spectra of CoO at two different photon energies with different incident angle, θ_i , with respect to the surface normal. The component of the electric field along the surface normal increases. Then the photoemission signals from $\Delta 1$ will increase and the photoemission signals from $\Delta 5$ initial state will decrease. The emission intensity of the feature *E* increase clearly as θ_i increase, indicating that the feature *E* has a $\Delta 1$ symmetry. The symmetry of the feature *D* is more difficult to see, mainly due to the influence of the feature *C*. However, relative to the intensity of the feature *A*, the lower panel of Fig. 7 shows that the intensity of the feature *D* decrease with the increase of θ_i , which suggests that it has a $\Delta 5$ symmetry. The $\Delta 5$ symmetry of the feature *D* can be more clearly seen in a published data by Brooks *et al.* (the spectrum of 55 eV photon energy in Fig. 2 of Ref. 17).

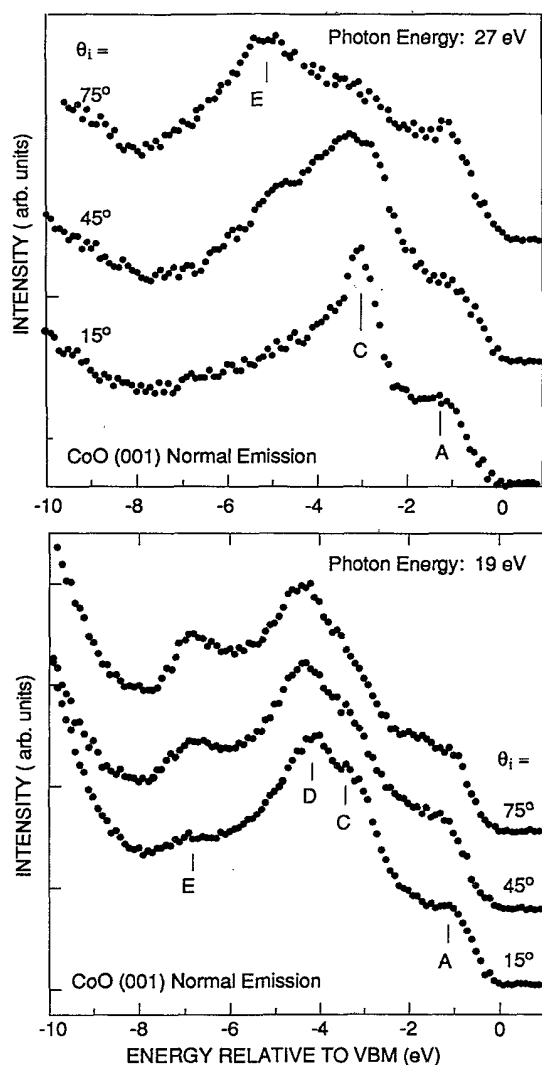


FIG. 7. Normal-emission angle-resolved photoemission spectra at two photon energies with three different photon incident angles. Feature *E* increases with the increase of incident angle, reflecting a $\Delta 1$ symmetry.

Using a free-electron final state with an effective mass of 0.98 and inner potential of -8 eV,¹⁷ we obtained an experimental *E* versus *k* relation from angle-resolved photoemission data including those presented in Fig. 6. Figure 8 presents the experimentally obtained *E* versus *k* relations together with theoretical bands from a nonmagnetic density functional band calculation.⁵⁸ The absolute energy position of the calculated bands is arbitrary, adjusted to give a best fit to the experimental data. Many things can be learned from this comparison. First of all, features *E* and *D* are corresponding to the $\Delta 1$ and $\Delta 5$ oxygen bands, and the experimental oxygen bands agree with the calculated bands excellently. This also agrees with the above symmetry discussions. The origin of the nondispersive feature *C* is not clear yet; two possible explanations are explained as follows: (a) It is due to a one-dimensional density of states connected to the high density of states of the 2' band at *X* point. Even though the 2' band is forbidden by the selection rule at normal emission, we think it is picked up by the finite (4°) angular resolution of our spectrometer. Similar features were also observed in NiO, MnO as well as transition-metal carbides, where they can also be best assigned as due to a one-dimensional density of states.^{16,59} (b) It is due to a dispersive Co 3*d* bands, as one would expect from a cluster configuration interaction model with crystal-field splitting similar to the case of NiO.¹⁵ For the Co 3*d* band (*A* band), however, unlike the oxygen bands, the experimental *E* versus *k* relation and the theoretical results do not agree with each other. Since we can only observe $\Delta 1$ and $\Delta 5$ bands at normal emission, the calculated width of these two bands is about 1.2 eV, while the experimental bandwidth observed in the dispersion is about 0.3 eV. Therefore, the observed 3*d* bandwidth is about 25% that of the calculated one. The narrowing of the cation 3*d*

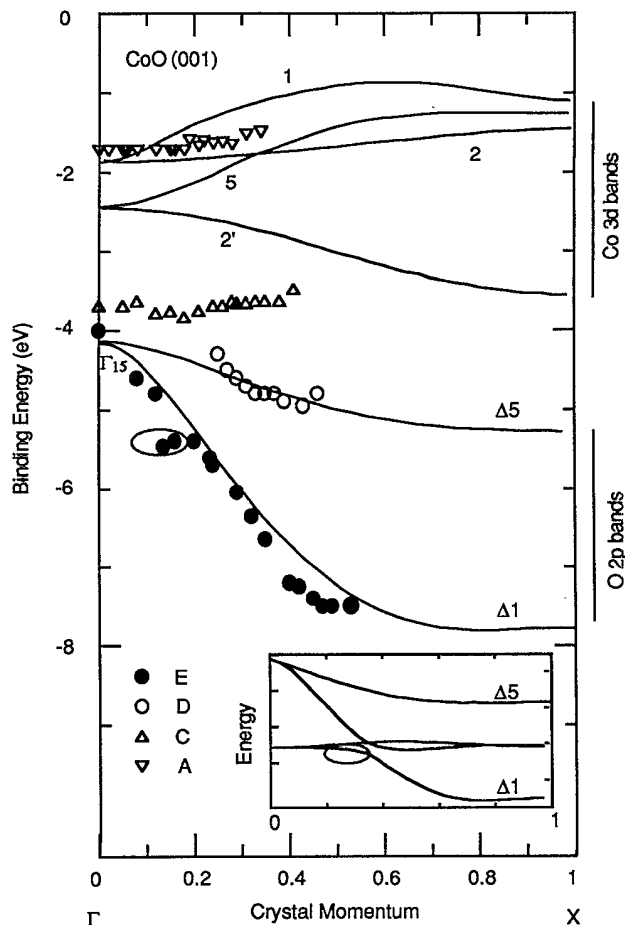


FIG. 8. Comparison of experimental E vs k relation with the results of a nonmagnetic band calculation (Ref. 58). The absolute position of the calculated bands is arbitrary.

bands is clearly a result of the strong correlation effects. Since the $3d$ bands are more close to the Fermi level, and the band theory fails to predict the $3d$ bands right, we believe that CoO is not a band insulator, which is consistent with angle-integrated photoemission data. From this figure, we get a mixed picture on the electronic structure of CoO. On the one hand, we have the data from oxygen bands that agree with the band calculation very well, and so does the energy separation between the $2p$ bands and $3d$ bands. On the other hand, we have data from Co $3d$ bands that do not agree with the band picture.

Brookes *et al.* have also performed an angle-resolved photoemission study of CoO.¹⁷ They claimed that they have found two d bands with different dispersions of 0.4 and 1.7 eV, respectively. Furthermore, they suggested that their experimental data are consistent with the band calculation in a broad term. We disagree with their interpretation of the experimental data, even though our data are consistent with theirs. The data presented in their paper were recorded at higher photon energies than ours, but the two sets of data have an overlap at 25 eV photon energy. The spectra obtained at $h\nu=25$ eV show the consistency of the two sets of data. The main source of

the discrepancy arises from the difficulty in the assignments of the various peaks. The uncertainty in determining the peak position of features A and C of Fig. 6 is pretty large, thus the error bars of data points of the features A and C in Fig. 8 are not very small, which is also true in their data. The main reason for us believe that the dispersions of the d bands are smaller than what they previously suggested is coming from the earlier NiO data,¹⁶ where the peak positions are much easier to be determined. The Ni bands accurately determined give much smaller d -band widths than 1.7 eV, hence we believe that the dispersions of the Co derived bands in CoO should also be smaller since one would expect that the dispersions of the Ni derived bands and the Co derived bands are very similar. Finally, a recent angle-resolved photoemission experiment from the MnO(100) surface gives at most ± 0.1 eV dispersion for the Mn d bands,⁶⁰ this again indicates that the dispersion of Co bands in the CoO are smaller than the 1.7 eV value. The other possible source of the discrepancy is that they are using a non self-consistent band calculation,⁶¹ which according to a self-consistent calculation underestimated the oxygen band width by about 1.5 eV.⁵⁸

Now let us come back and discuss the reasons why we believe that feature E has two branches at photon energies higher than 26 eV, below which the assignments of the peaks is very unambiguous. At photon energies higher than 26 eV, it is clear that feature E turns slightly back to lower energy (or at least one can say it stops to move towards high energy), as indicated by the points circled out. For the following reasons, we believe that it has another branch continue to move toward higher energy as indicated. (a) If it does not have another branch, then it means that a critical point has been reached and the point corresponding to photon energy of 26 or 27 eV should be the Γ point in k space, but the k value obtained for peak E at the photon energy of 26 eV is $0.2G_{\Gamma X}$. To convince ourselves, we have also tried to interpret our data by assuming this is a band critical point, which results in a very unrealistic inner potential or effective mass for the final state. (b) If it does not have another branch and the slightly back bending of the feature is caused by reaching the Γ point, then the bandwidth of the $\Delta 1$ band is only about 2.2 eV. This is about 1.5 eV narrower than the oxygen bandwidth from a self-consistent band calculation.⁵⁸ Since we expect that the band calculation will give a very reasonable account of the oxygen bands, this is not very likely. (c) This is the best way to give a coherent picture for angle-resolved photoemission data from NiO, CoO, and MnO.¹⁶ Especially in the NiO data, two branches of the feature E can clearly be seen at photon energies of 27 and 28 eV. Given the similarity between NiO and CoO, we are confident that the way we interpret our data is correct. In order to understand this back bending, we present the $\Delta 1$ and $\Delta 5$ bands from a magnetic calculation as an inset of the Fig. 8.⁵⁸ The main effect of including the AF order in the band calculation is the small splitting of the $\Delta 1$ band. We believe the slight back bending (or fluttering) branch is due to the effects from the AF order. Even though the experimental data were collected at room temperature where CoO is in its

paramagnetic phase, local antiferromagnetic order persists above its Neel temperature which can define a local antiferromagnetic bands, as pointed out in Sec. IV. This can also explain the observation that the magnetic splitting of the $\Delta 1$ band is more clearly seen in NiO data which were collected well below its Neel temperature than in CoO data which were recorded just above its Neel temperature.¹⁶ It should be emphasized that the effects of the antiferromagnetic order on the oxygen bands are much weaker than that on Co bands since the moments are located on the Co sites. Because we have seen the effects of magnetic order on oxygen bands, we suggest that the effects of the magnetic order on the Co bands are very strong. Before leaving this subject, we would like to point out that feature *D* also merges with feature *C* at photon energies near 27 eV, this can be seen in the upper panel of Fig. 7. At 15° incident angle, the intensity from feature *C* enhances dramatically, which can be explained by the fact feature *D* merges with features *C* and *D* ($\Delta 5$ symmetry) enhances at lower incident angle.

We can learn many interesting things from the results presented in Fig. 8. First of all, it clearly shows that the fundamental difference between Co *3d* and O *2p* bands lies in their energy bandwidth. The total bandwidth (listed in Table II), W , for the oxygen bands is about 4 eV while that of the Co bands is about 0.3 eV. Using the U_d and U_p values presented in Table II, we obtain U/W values of 30 and 1.5 for Co *3d* and O *2p* bands, respectively. For O *2p* bands, our data show that the one-electron band theory gives a good description of them, which is not a straightforward conclusion one would draw from the about 1.5 U/W ratio. A possible explanation for this interesting observation is that the oxygen bands are very close to a full-band situation where the correlation effect is irrelevant to the single-hole created by the photoemission process. This explanation, however, has a difficulty to reconcile the fact that there are very extensive hybridizations between Co *3d* and O *2p* states. As a result of these hybridizations, O *2p* states are not completely filled. More experimental and theoretical efforts are needed to clarify this important observation. In the same context, we would like to emphasize that the intrinsic oxygen bandwidth (i.e., the oxygen-oxygen direct overlapping) is important, which is also realized in the high- T_c superconducting compounds.⁶² For the Co *3d* bands, $U/W \gg 1$, one-electron band picture breaks down and a more localized model such as the Hubbard or the Anderson Hamiltonian is a more appropriate approach. Referenced to their energy bandwidths, the $U_d \rightarrow \infty$, and $U_p \rightarrow 0$ limit might be a reasonable approximation, which may provide justifications for the slave boson approaches used in similar materials.^{63–65} Secondly, we see that the effects of the local magnetic order have to be taken into account. In the field of high-temperature superconductivity, there are increasing numbers of experimental evidence that the local magnetic order persists,^{66,67} the influence of the local magnetic order on the electron structure has been explored theoretically also.⁶⁸ Our observation emphasizes the importance of such efforts.

The most important implication of our finding is that it

gives a general guideline for theoretical efforts to calculate the band structures of CoO. In the field of using angle-resolved photoemission to study the electronic structure of solids, a lot of efforts have been put in to correct the discrepancies between the experimental quasi-particle spectra and the one-electron eigenvalues of the band calculations by the self-energy correction with GW approximation, where only the first term of the self-energy operator is taken to represent the entire interaction.^{69–72} For simple metals like Na, this procedure works well in explaining the difference in the experimental bandwidth and results of one-electron band calculations.^{69,70} This suggests that the self-energy effects are generally important in analyzing photoemission data. For semiconductors like Ge and Si, the self-energy correction is essential to obtain the right energy gaps.⁷¹ Even for Ni metal, Liebsch has used this approach to account the strong *d-d* correlation effects.⁷² Starting with the degenerate Hubbard model and using a low-density approximation for *d* holes, Liebsch can semiquantatively explain the features of Ni photoemission spectra which cannot be reconciled with the one-electron band model: (1) The shake-up structure observed at about 6 eV below the Fermi energy; (2) the *3d* band is about 25% smaller than that predicted theoretically; (3) the exchange splitting in ferromagnetic Ni is approximately half as that derived from the band theory. The narrowing of the Ni *3d* band is mainly due to its shifting towards E_F as a result of the fact that the self-energy decreases roughly linearly with the binding energy. Very recently, self-energy correction approach has also been used to calculate angle-resolved photoemission spectra of Ni metal. Including a full self-energy correction (i.e., with energy-dependent real and imaginary parts for the self-energy), Jordan *et al.* find a good agreement between the calculated and the experimental spectra from the Ni(110) surface.⁷³ Experiencing these successes in using self-energy correction to explain the photoemission data, one would attempt to use a similar tactic to explain the photoemission data of highly correlated materials like CoO and NiO. Presently, little work has been done to use the self-energy approach to explain the photoemission data from the highly correlated materials. The constant self-energy correction for NiO is the only example we are aware of,⁷⁴ which is obviously over simplified and cannot explain the photoemission data. If one starts from a one-electron band calculation and then modifies the calculated bands by self-energy correction, then one has to introduce a mechanism that reduces Co *3d* bandwidth by a factor of 25% or so while still retaining the other essential features of the band calculation. On the other hand, one may also start out from a cluster calculation and then try to incorporate in the dispersion. However, the practical ways to perform these calculations and the validities of these calculational approaches remain to be seen.

VI. SUMMARY

From the experimental data, we have seen two aspects of the electronic structure of CoO. On the one hand,

strong correlation effects were observed, which appear in the form of satellites at high binding energy and strong narrowing of the Co 3d bands. The Co 3d nature of the valence-band satellite is verified by its resonance behavior. We interpret our resonance photoemission data in terms of a cluster configuration interaction model. CoO is a charge-transfer insulator, with about 6 eV energy gap and 9–11 eV Coulomb interaction energy, U_d . On the other band, strong indications of band effects were observed for the oxygen states in the angle-resolved photoemission data. The dispersions of the oxygen bands agree with the results of one electron band calculation almost perfectly. Effects of "local antiferromagnetic order" on the electronic structure must be considered in order to reconcile angle-resolved photoemission data, which receives its support from results of XPS study at different temperatures.

ACKNOWLEDGMENTS

One of us (Z.X.S.) would like to thank Dr. O. Jepsen and R. Kasowski for many discussions. They have also sent us their calculations on NiO and CoO before publication. The experiment was performed at SSRL which is funded by the Department of Energy (DOE) under Contract No. DE-AC03-82ER-13000, Office of Basic Energy Science, Division of Chemical/Material Science. The Los Alamos work was funded by DOE. We express thanks for support from the National Science Foundation (NSF) Contract No. DMR-89103478, The United States Joint Services Electronics Program (JSEP) Contract No. DAAG 29-85-K-0048, and the U.S. National Science Foundation through the Low Temperature Physics Grants No. DMR-87-21654 (J.S.K. and J.W.A.). Two of us also would like to acknowledge support from the NSF (D.S.D.) and from the Norwegian Council for Research and the Humanities (A.B.).

- ¹J. G. Bednorz and K. A. Muller, *Z. Phys. B* **64**, 189 (1986).
- ²See, e.g., W. E. Pickett, *Rev. Mod. Phys.*, **61**, 443 (1989).
- ³P. W. Anderson, in *Frontiers and Borderlines in Many Particle Physics*, Proceedings of the International School of Physics, "Enrico Fermi" (North-Holland, Amsterdam, in press).
- ⁴B. H. Brandow, *Adv. Phys.* **26**, No. 5, 651 (1977).
- ⁵N. F. Mott, *Proc. R. Soc. London, Ser. A* **62**, 416 (1949).
- ⁶J. Hubbard, *Proc. R. Soc. London, Ser. A* **276**, 238 (1963).
- ⁷P. W. Anderson, *Phys. Rev.* **115**, 2 (1959).
- ⁸G. A. Sawatzky and J. W. Allen, *Phys. Rev. Lett.* **53**, 2339 (1985).
- ⁹J. Zaanen, G. A. Sawatzky, and J. W. Allen, *Phys. Rev. Lett.* **55**, 418 (1985).
- ¹⁰J. C. Slater, *Phys. Rev.* **82**, 538 (1951).
- ¹¹K. Terakura, T. Oguchi, A. R. Williams, and J. Kübler, *Phys. Rev. B* **30**, 4734 (1984); T. Oguchi, K. Terakura, and A. R. Williams, *ibid.* **28**, 6443 (1983).
- ¹²R. J. Powell and W. E. Spicer, *Phys. Rev. B* **2**, 2182 (1970).
- ¹³C. Kittel, *Introduction to Solid State Physics* (Wiley, New York, 1953).
- ¹⁴See, for example, M. D. Reichtin, S. C. Moss, and B. L. Averbuch, *Phys. Rev. Lett.* **24**, 395 (1975).
- ¹⁵A. Fujimori and F. Minami, *Phys. Rev. Lett.* **53**, 2339 (1985); *Phys. Rev. B* **30**, 957 (1984).
- ¹⁶Z. X. Shen, Ph.D. thesis, Stanford University, 1989; Z.-X. Shen, C. K. Shih, O. Jepsen, I. Lindau, W. E. Spicer, and J. W. Allen, *Phys. Rev. Lett.* **64**, 2442 (1990).
- ¹⁷N. B. Brookes, D. S.-L. Law, D. R. Warburton, P. L. Wincott, and G. Thornton, *J. Phys. Condens. Matter* **1**, 4267 (1989).
- ¹⁸K. S. Kim, *Phys. Rev. B* **11**, 2177 (1975).
- ¹⁹D. E. Eastman and J. L. Freeouf, *Phys. Rev. Lett.* **34**, 395 (1975).
- ²⁰S. Hüfner and G. K. Wertheim, *Phys. Rev. B* **8**, 4857 (1973).
- ²¹T. Oguchi, K. Terakura, and A. R. Williams, *Phys. Rev. B* **28**, 6443 (1983).
- ²²A. Fujimori, K. Terakura, M. Taniguchi, S. Ogawa, S. Suga, M. Matoba, and S. Anzai, *Phys. Rev. B* **37**, 3109 (1988).
- ²³R. J. Powell and W. E. Spicer (unpublished).
- ²⁴A. Fujimori, N. Kimizuka, M. Taniguchi, and S. Suga, *Phys. Rev. B* **36**, 6691 (1987).
- ²⁵S. J. Oh, J. W. Allen, I. Lindau, and J. C. Mikkelsen, Jr., *Phys. Rev. B* **26**, 4845 (1982).
- ²⁶M. R. Thüler, R. L. Benbow, and Z. Hurych, *Phys. Rev. B* **26**, 669 (1982).
- ²⁷R. L. Kurtz, R. C. Stockbauer, D. Mueller, A. Shih, L. E. Toth, M. Osofsky, and S. E. Wolf, *Phys. Rev. B* **36**, 8818 (1987).
- ²⁸Z.-X. Shen, J. W. Allen, J. J. Yeh, J. S. Kang, W. Ellis, W. E. Spicer, I. Landau, M. B. Maple, Y. D. Dalichaouch, M. S. Torikachvili, J. Z. Sun, and T. H. Geballe, *Phys. Rev. B* **36**, 8414 (1987).
- ²⁹P. Thirty, G. Rossi, Y. Petroff, A. Revcolevschi, and J. Jegoudez, *Europhys. Lett.* **5**, 55 (1988).
- ³⁰P. D. Johnson, S. L. Qiu, L. Jiang, M. W. Euckman, Myron Strongin, S. L. Hurlbert, R. F. Garrett, B. Sinkovic, N. V. Smith, R. J. Cava, C. S. Jee, N. Nichols, E. Kaczanowicz, R. E. Salomon, and J. E. Crow, *Phys. Rev. B* **35**, 8811 (1987).
- ³¹S. Hüfner and G. K. Wertheim, *Phys. Rev. B* **7**, 5086 (1973).
- ³²K. Terakura, A. R. Williams, T. Oguchi, and J. Kübler, *Phys. Rev. Lett.* **52**, 1983 (1984).
- ³³J. Zaanen and G. A. Sawatzky, *Can. J. Phys.* (to be published).
- ³⁴G. van der Laan, C. Westra, C. Haas, and G. A. Sawatzky, *Phys. Rev. B* **23**, 4369 (1981).
- ³⁵See, for example, the relation of U_{cd} (noted as Q) and U_d in Ni dihalides, J. Zaanen, C. Westra, and G. A. Sawatzky, *Phys. Rev. B* **33**, 8060 (1986), also the relation between U_{cd} and U_d in various Cu compounds as presented in Ref. 28.
- ³⁶S.-J. Oh *et al.* (unpublished).
- ³⁷It should be noted that it is more difficult to determine the positions of Co 3s and Co 3p satellite positions because of the complications of the multiple splittings of the main lines. The values listed in Table I are best estimates.
- ³⁸A. J. Blodgett, Jr. and W. E. Spicer, *Phys. Rev. Lett.* **15**, 29 (1965).
- ³⁹C. S. Fadley and D. A. Shirley, compiled by J. W. D. Connolly, in *Electronic Density of States*, Natl. Bur. Stand. (U.S.) Circ. No. 3223 (U.S. GPO, Washington, D.C., 1971).
- ⁴⁰L.-G. Peterson, R. Melander, D. P. Spears, and S. B. M. Hagström, *Phys. Rev. B* **14**, 4177 (1976).
- ⁴¹J. C. Slater, *J. Appl. Phys.* **39**, 761 (1968).
- ⁴²J. Hubbard, *Phys. Rev. B* **19**, 2626 (1979); You and Heine, *J. Phys. F* **12**, 177 (1982); Hasegawa, *J. Phys. Soc. Jpn.* **49**, 963 (1980).

- (1980); W. A. Harrison, *Solid State Theory* (McGraw-Hill, New York, 1970).
- ⁴³D. E. Eastman, F. J. Himpsel, and J. A. Knapp, *Phys. Rev. Lett.* **40**, 1514 (1978).
- ⁴⁴E. P. Wahlfarth, *Phys. Lett.* **36A**, 131 (1971).
- ⁴⁵H. Capellmann, *J. Phys. F* **4**, 1466 (1974); *Z. Phys. B* **34**, 29 (1979).
- ⁴⁶H. Capellmann, *Solid State Commun.* **30**, 7 (1979).
- ⁴⁷V. Korenman, J. L. Murray, and R. E. Prange, *Phys. Rev. B* **16**, 4032; **16**, 4048 (1980); **16**, 4058 (1980).
- ⁴⁸T. Moriya, *J. Magn. Magn. Mater.* **14**, 1 (1979).
- ⁴⁹H. Capellmann and R. E. Prange, *Phys. Rev. B* **23**, 4709 (1981).
- ⁵⁰H. Hopster, R. Raue, G. Guntherodt, E. Eisker, R. Clamberg, and M. Campagna, *Phys. Rev. Lett.* **51**, 829 (1983).
- ⁵¹E. Eisker, K. Schröder, M. Campagna, and W. Gudat, *Phys. Rev. Lett.* **52**, 2285 (1984).
- ⁵²B. Hermseier, J. Osterwalder, D. J. Freidman, and C. S. Fadley, *Phys. Rev. Lett.* **62**, 478 (1989).
- ⁵³B. Sinkovic, B. Hermseier, and C. S. Fadley, *Phys. Rev. Lett.* **55**, 1227 (1985).
- ⁵⁴B. Hermseier (unpublished).
- ⁵⁵N. V. Smith and F. J. Himpsel, in *Handbook on Synchrotron Radiation*, edited by E.-E. Koch (North-Holland, Amsterdam, 1983), Chap. 9.
- ⁵⁶J. Hermanson, *Solid State Commun.* **22**, 9 (1977).
- ⁵⁷W. Eberhardt and F. J. Himpsel, *Phys. Rev. B* **21**, 5572 (1980).
- ⁵⁸O. Jepsen (unpublished).
- ⁵⁹P. A. P. Lindberg, Ph.D. thesis, Linchopin University, Sweden, 1988.
- ⁶⁰Robert J. Lad and Victor E. Henrich, *Phys. Rev. B* **38**, 10 860 (1988).
- ⁶¹L. F. Matheiss, *Phys. Rev. B* **5**, 290 (1972).
- ⁶²A. K. McMahan, R. M. Martin, and S. Satpathy, *Phys. Rev. B* **38**, 6650 (1988).
- ⁶³D. M. Newns, Mark Rasolt, and P. C. Pattnaik, *Phys. Rev. B* **38**, 6513 (1988); D. M. Newns, P. C. Pattnaik, M. Rasolt, and D. A. Papaconstantopoulos, *Phys. Rev. B* **38**, 7033 (1988).
- ⁶⁴P. A. Lee, G. Kottiar, and N. Read, *Physica B+C* **148B**, 274 (1987).
- ⁶⁵C. A. R. Sa'De Melo and S. Doniach, *Phys. Rev. B* **41**, 6633 (1990).
- ⁶⁶Robert J. Birgeneau and Gen Shirane, in *Physical Properties of High Temperature Superconductors*, edited by D. M. Ginsberg (World Scientific, Singapore, in press).
- ⁶⁷P. C. Hammel, M. Takigawa, R. H. Hoffner, Z. Fisk, and K. C. Ott, *Phys. Rev. Lett.* **63**, 1992 (1989).
- ⁶⁸A. Kampf and J. R. Schrieffer, *Phys. Rev. B* **41**, 6399 (1990).
- ⁶⁹H.-J. Freund, W. Eberhardt, D. Heskett, and E. W. Plummer, *Phys. Rev. Lett.* **50**, 768 (1983); In-Whan Lyo and E. W. Plummer, *ibid.* **60**, 1558 (1988).
- ⁷⁰Kenneth W.-K. Shung, B. E. Sernelins, and G. D. Mahan, *Phys. Rev. B* **36**, 4499 (1987).
- ⁷¹W. Jackson and J. W. Allen, *Phys. Rev. B* **37**, 4618 (1988), and references therein.
- ⁷²Ansgar Liebsch, *Phys. Rev. Lett.* **43**, 1431 (1979).
- ⁷³R. G. Jordan and M. A. Hoyland (unpublished).
- ⁷⁴J. Kubler and A. R. Williams, *J. Magn. Magn. Mater.* **54-57**, 603 (1986).